International Journal of Oral Science (2017) 9, 74–79
www.nature.com/ijos

OPEN

ORIGINAL ARTICLE

Biofilm three-dimensional architecture influences *in situ* pH distribution pattern on the human enamel surface

Jin Xiao[1], Anderson T Hara[2], Dongyeop Kim[3], Domenick T Zero[2], Hyun Koo[3] and Geelsu Hwang[3]

To investigate how the biofilm three-dimensional (3D) architecture influences *in situ* pH distribution patterns on the enamel surface. Biofilms were formed on human tooth enamel in the presence of 1% sucrose or 0.5% glucose plus 0.5% fructose. At specific time points, biofilms were exposed to a neutral pH buffer to mimic the buffering of saliva and subsequently pulsed with 1% glucose to induce re-acidification. Simultaneous 3D pH mapping and architecture of intact biofilms was performed using two-photon confocal microscopy. The enamel surface and mineral content characteristics were examined successively *via* optical profilometry and microradiography analyses. Sucrose-mediated biofilm formation created spatial heterogeneities manifested by complex networks of bacterial clusters (microcolonies). Acidic regions (pH < 5.5) were found only in the interior of microcolonies, which impedes rapid neutralization (taking more than 120 min for neutralization). Glucose exposure rapidly re-created the acidic niches, indicating formation of diffusion barriers associated with microcolonies structure. Enamel demineralization (white spots), rougher surface, deeper lesion and more mineral loss appeared to be associated with the localization of these bacterial clusters at the biofilm-enamel interface. Similar 3D architecture was observed in plaque-biofilms formed *in vivo* in the presence of sucrose. The formation of complex 3D architectures creates spatially heterogeneous acidic microenvironments in close proximity of enamel surface, which might correlate with the localized pattern of the onset of carious lesions (white spot like) on teeth.
International Journal of Oral Science (2017) **9,** 74–79; doi:10.1038/ijos.2017.8; published online 28 April 2017

Keywords: biofilms; demineralization; dental caries; exopolysaccharides; microcolonies; pH microenvironments; plaque; *Streptococcus mutans*

INTRODUCTION

Dental caries is currently one of the most widespread oral infectious diseases associated with a biofilm known as dental plaque. The term caries is used to describe the signs of a localized chemical dissolution of the tooth enamel surface caused by metabolic events taking place within the biofilm formed on the affected area.[1] Cariogenic biofilm develops when bacteria accumulate on the tooth surface often enmeshed in an exopolysaccharides (EPS)-rich matrix. Carbohydrate fermentation by microorganisms embedded in a diffusion-limiting EPS-rich matrix leads to organic acid accumulation locally, which causes acidification of the extracellular milieu. This causes a variation in the degree of saturation of fluid phase of plaque with respect of hydroxyapatite leading to enamel acid-dissolution. Therefore, dental caries is the direct consequence of the localized acidic pH microenvironments across the biofilm structure and at the tooth-biofilm interface.[2]

A myriad of different approaches have been developed to determine pH values in dental plaque *in situ*.[3] Previously, pH electrodes constructed from antimony or glass, iridium or field effect transistors were widely used.[4] However, the use of contact electrodes requires disruption of plaque integrity, and they are not sensitive to localize pH, specifically at the plaque-tooth interface.[5–6] Indwelling glass electrodes can determine the average pH values at the interface[7–8] but are limited in measuring or localizing acidic pH values within the biofilm structure or across the enamel surface. Therefore, these techniques lack the capability to assess the heterogeneity of pH distribution within biofilms and at the apatite interface or the dynamic pH changes locally over time. Alternatively, advances in fluorescence chemistry have led to the development of pH sensitive dyes or probes, such as carboxyfluorescein,[9] C-SNARF-4,[10] Lysosensor yellow/blue,[11] pHluorin[12] and nanosensor[13] that can be used together with confocal microscopy and computational analysis. These approaches enabled *in situ* pH measurement without compromising the biofilm architecture, revealing heterogeneous and localized pH distribution within *in vitro* biofilms.[11–13]

Despite the critical importance of acidic microenvironments formed in the plaque-biofilm in causing the enamel demineralization, little is known about how the biofilm structure influences the acidification of the milieu and demineralization of the enamel surface. Here, we applied

[1]Eastman Institute for Oral Health, University of Rochester Medical Center, Rochester, USA; [2]Department of Cariology, Operative Dentistry and Dental Public Health, Oral Health Research Institute, Indiana University School of Dentistry, Indianapolis, USA and [3]Biofilm Research Laboratories, Levy Center for Oral Health, Department of Orthodontics and Divisions of Pediatric Dentistry & Community Oral Health, School of Dental Medicine, University of Pennsylvania, Philadelphia, USA
Correspondence: Dr J Xiao, Eastman Institute for Oral Health, University of Rochester Medical Center, 625 Elmwood Avenue, Rochester NY 14620, USA
E-mail: jin_xiao@urmc.rochester.edu
Dr G Hwang, Biofilm Research Laboratories, Levy Center for Oral Health, Department of Orthodontics and Divisions of Pediatric Dentistry & Community Oral Health, School of Dental Medicine, University of Pennsylvania, 240 S 40th Street, Levy Building RM 418, Philadelphia PA 19104, USA
E-mail: geelsuh@upenn.edu
Accepted 14 February 2017

our developed *in situ* pH mapping method[11] to assess the pattern and localization of acidic pH values throughout the biofilm architecture and across the enamel surface at the biofilm-apatite interface.

MATERIALS AND METHODS

Biofilm preparation

Sterilized enamel blocks (3 mm × 3 mm) were coated with sterile clarified saliva (sHA). Cells of 10^2 *Streptococcus mutans (S. mutans)* UA159 (ATCC 700610) were grown in buffered tryptone yeast-extract broth, pH 7.0 containing: (i) 1% sucrose; and (ii) 0.5% glucose+0.5% fructose. Biofilms were formed on enamel blocks mounted vertically in batch cultures at 37 °C in 5% CO_2 for 67 h as described elsewhere;[14–15] the culture medium was replaced twice daily. Biofilms were removed at 43 h and 67 h for three-dimensional (3D) structural and pH distribution analysis, the enamel slabs were collected for hard surface analysis including (i) surface roughness measurement and (ii) transversal microradiographic analysis.

Surface roughness measurement

A 2 mm × 2 mm area on the center of the specimen surface was scanned by a 3D optical profilometer (Proscan 2000, Scantron, Taunton, UK) using a chromatic sensor (S5/03), with a step size set at 0.01 mm, for 200 steps. All scans were completed using a frequency of 100 Hz with full sensor speed (100%). The value was averaged from two readings at each measuring point. The Ra (arithmetic average of absolute values) roughness parameter was measured on both *x* and *y* directions using dedicated software (Proscan 2000, Scantron, Taunton, UK).

Transversal microradiographic analysis

Specimens were mounted on plastic rods and sectioned with a hard tissue microtome (Silverstone-Taylor Hard Tissue Microtome, Series 1000 Deluxe, Scientific Fabrications Laboratories, Lafayette, CO, USA). One 100-μm section was obtained from the center of each specimen, mounted on x-ray sensitive plates (MicrochromeTechnology, San Jose, CA, USA) and subjected to X-ray, along with an aluminum step wedge. Microradiographic images were analyzed with dedicated software (Inspektor TMR 2000, ver.1.25, Inspektor Research Systems BV, Amsterdam, The Netherlands) with sound enamel defined at 87% mineral volume to obtain mean lesion depth (μm).

Laser scanning confocal fluorescence microscopy imaging of biofilms

The 3D structure and spatial distribution of EPS and bacterial cells within intact *in vitro* biofilms was determined using optimized protocols for biofilm imaging *via* multi-photon confocal fluorescence microscopy.[16] Briefly, 1 μmol · L^{-1} Alexa Fluor 647-labeled dextran conjugate (molecular weight, 10 kDa; absorbance/fluorescence emission maxima of 647/668 nm; Molecular Probes, Invitrogen, Carlsbad, CA, USA) was use to label the EPS matrix of the biofilms. This fluorescent dextran added to the culture medium probe serves as a primer for Gtfs and can be directly incorporated into newly formed glucans during synthesis of EPS matrix over the course of biofilm development. All the bacterial species were stained with SYTO 9 green fluorescent nucleic acid stain (485/498 nm; Molecular Probes) using standard protocols.[15–17] The imaging was performed using an Olympus FV 1000 two-photon laser scanning microscope (Olympus, Tokyo, Japan) equipped with a 10× (0.45 numerical aperture) or 25× LPlan N (1.05 numerical aperture) water immersion objective lens. The excitation wavelength was 810 nm, and the emission wavelength filter for SYTO 9 was a 495/540 OlyMPFC1 filter, while the filter for Alexa Fluor 647 was an HQ655/40M-2P filter. Each enamel block was removed at 43 h and 67 h and scanned at each corner of the block which including four scanning windows. Three independent biofilm experiments were performed. The three-dimensional architecture of the biofilms was visualized using Amira 5.0.2 (Mercury Computer Systems, Chelmsford, MS, USA).

Non-invasive 3D *in situ* pH measurement and visualization

The ability to characterize microenvironments (for example, spatial pH distribution) within biofilms without disrupting their architectural integrity is a major technical challenge. We used a fluorescent pH indicator, Lysosensor yellow/blue (Molecular Probes), to determine the *in situ* pH in our biofilm model. Lysosensor yellow/blue is conjugated with dextran (10 kDa MW), which allows the labeled dextran to be directly incorporated into the EPS matrix,[16] as described previously. Once incorporated into the biofilm matrix, the pH values can be measured based on fluorescence intensity ratio of the dual-wavelength fluorophore.[18] Lysosensor yellow/blue exhibits a dual-emission spectral peak (fluorescence emission maxima 452 and 521 nm) that is pH dependent.[18] The pH measurements are based on the principle that protonation of the fluorophore shifts its emission spectra, such that increasing ion concentrations increase fluorescence intensity at one wavelength, while decreasing it at the other.[19] The fluorescence intensity of both emission wavelengths and the ratio of fluorescent intensity (I450/I520) within each biofilm confocal image were measured using Image J 1.44 and its calculation tools (for example, channel 1 divided by channel 2 as detailed in http://rsbweb.nih.gov/ij/download.html). Titration curves of ratios *vs* pH (ranging from 3.5 to 7.0) were calculated as described previously,[19] and were used to convert Lysosensor yellow/blue emission (fluorescence intensity) ratios to pH values. Lysosensor yellow/blue is particularly suitable for acidic environments (low sensitivity maximum; pKa ~ 4.2), as expected in our biofilm model.[18]

The confocal images of lysosensor-incorporated biofilms were acquired before and after incubation in Na_2HPO_4-citric acid buffer at pH 7.0. The images were acquired after 15, 30, 45, 60 and 120 min of incubation in the neutral buffer to evaluate the spatial distribution of pH across the intact 3D biofilm architecture. After 120 min total neutralization, 1% glucose (final concentration) was introduced into the medium and the re-acidification within the biofilm structure was observed. For pH measurement, the ratio of fluorescence intensity of selected areas within each biofilm image were converted to pH values using the titration curves and Image J software (http://www.uhnresearch.ca/facilities/wcif/PDF/ImageJ_Manual.pdf). For visualization of *in situ* pH distribution within the 3D biofilm architecture, the fluorescence intensity ratios (corresponding to the pH values between 7.0 and 3.5) of all confocal images were reconstructed using Image J, then Amira. The fluorescence intensity was converted into gray scale using the Amira toolbox to correlate with the pH range from 7.0 (white) to 3.5 (black). Unlabeled biofilms were also imaged to check whether the autofluorescence of each biological component of the biofilm (*i.e.* bacterial cells and glucans) would interfere with pH quantification at the wavelengths used in our study; there was no interference with the measurements based on our image analysis.

Fluorescence *in situ* hybridization of *in vivo* formed plaque-biofilm

Furthermore, we also examined the 3D architecture of multispecies biofilms formed during exposure to sucrose or glucose+fructose on enamel specimens placed in the mouth using a modified intra-oral caries model[20–22] according to approved institutional review board (IRB) protocol at Indiana University (IRB #1407637739). Briefly, subjects wore their partial denture with two flattened and polished enamel specimens imbedded in the buccal surface of the posterior denture teeth for 14 days. The enamel specimens were previously

inserted in plastic holders designed to create a 0.5 mm recess from the denture surface to encourage biofilm formation of standardized thickness. The subjects were randomly assigned to the experimental groups (20% sucrose solution, 10% glucose+10% fructose solution, or distilled water (negative control)). On each test day, subjects applied 1 ml of the assigned test solution on the enamel specimen for 1 min, 4× per day. Subjects wore the study partial denture 24 h per day, except during meals and brushing of their natural teeth. After 14 days, the enamel specimens were carefully removed from the partial dentures avoiding biofilm detachment and disruption, and prepared for biofilm 3D architecture analysis *via* fluorescence *in situ* hybridization (FISH) as described elsewhere.[23–24] Briefly, the intact biofilms formed on enamel specimens were gently washed twice with phosphate-buffered saline (PBS), and fixed with 4% paraformaldehyde (in PBS, pH 7.4) at 4 °C for 4 h, at which point the fixed cells were washed trice with PBS. After washing, sample was transferred into 50% ethanol (in PBS, pH 7.4) and stored at −20 °C. FISH oligonucleotide probes used in this study as follows: EUB338, 5′-GCTGCCTCCCGTAGGAGT-3′ with Cy3 for all eubacteria; STR405, 5′-TAGCCGTCCCTTTCTGGT-3′ with Cy5 for *Streptococcus*. The sample in the hybridization buffer (30% formamide, 0.9 mol · L^{-1} NaCl, 0.01% SDS, 20 mmol · L^{-1} Tris-HCl, pH 7.2) with the probes was incubated at 46 °C for 2 h. After the incubation, the hybridized cells were washed with wash buffer (0.2 mol · L^{-1} NaCl, 20 mmol · L^{-1} Tris-HCl (pH 7.5), 5 mmol · L^{-1} EDTA, 0.01% sodium-dodecyl sulphate (SDS)) and further incubated 46 °C for 10 min. The 3D biofilm architecture was acquired using multi-photon confocal laser scanning microscope (SP5, Leica Microsystems, Buffalo Grove, IL, USA) equipped with a ×20 (1.0 numerical aperture) water immersion lens. The biofilm were sequentially scanned using the 543 nm and 633 He-Ne lasers and the fluorescence emitted was collected with the internal spectral detectors (PMT3 (540–580 nm) for Cy3 and PMT4 (680–720 nm) for Cy5, respectively). High resolution (1 024 × 1 024 pixels) and high magnification images were acquired using an inverted confocal laser scanning microscope (SP5-II, Leica Microsystems) equipped with a ×63 (1.4 numerical aperture) oil immersion lens with ×2 zoom. The biofilms were sequentially scanned using the 543 nm and 633 nm He-Ne lasers, and the fluorescence emitted was collected with the hybrid detector (550–653 nm for Cy3 and 644–752 nm for Cy5, respectively). Amira 5.4.1 software (Visage Imaging, San Diego, CA, USA) was used to create 3D renderings to visualize the architecture of the biofilms.

Statistical analysis

The data were analyzed using analysis of variance, and the F-test was used to test any difference among the test groups. When significant differences were detected, pairwise comparisons were made between all the groups using Tukey's method to adjust for multiple comparisons. Statistical software JMP version 3.1 (SAS Institute, Cary, NC, USA) was used to perform the analyses. The level of significance was set at 5%.

RESULTS

Biofilm 3D architecture and enamel hard surface characteristics

The biofilm 3D architecture and enamel hard surface characteristics are shown in Figure 1. Distinct biofilm structure was observed

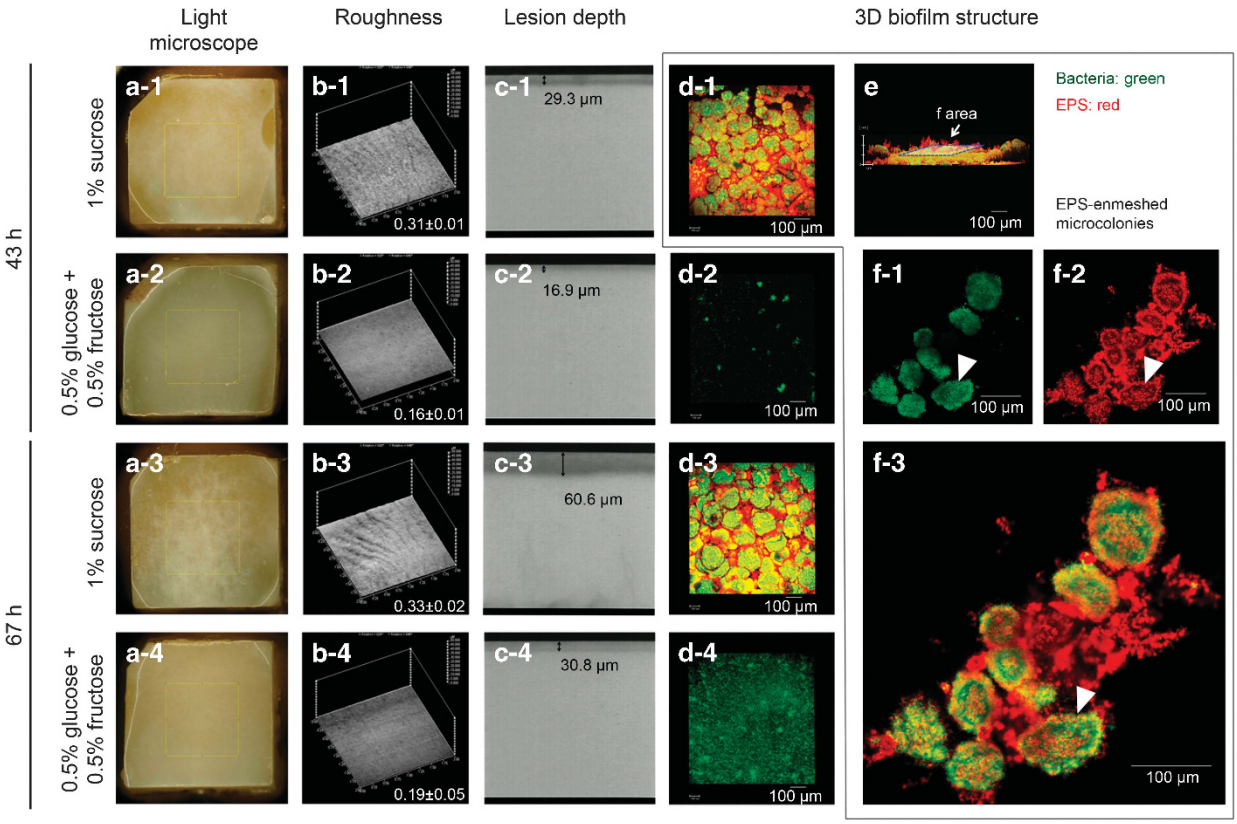

Figure 1 Biofilm structure and Enamel hard surface characteristics. Light microscopic images (**a**-1-**a**-4), enamel roughness (**b**-1-**b**-4), lesion depth of the enamel (**c**-1-**c**-4) and 3D reconstructed confocal microscopic images (**d**-1-**d**-4) were shown. A selected sectional image of the biofilm formed in 1% sucrose (**d**-1) was shown in (**e**) and (**f**-1-**f**-3). The white arrow labeled in images (**f**-1-**f**-3) indicated the microcolony structure in the biofilms. 3D, three-dimensional; EPS, exopolysaccharides.

between 1% sucrose and 0.5% glucose+0.5% fructose groups during biofilm development (Figure 1d). In glucose+fructose biofilm, only small cell clusters were detected at 43 h (Figure 1d-2); the bacteria coverage on enamel surface increased from 43 h to 67 h (Figure 1d-4), while EPS was not visible at both time point. In contrast, biofilm formed in 1% sucrose revealed intricate and complex structure with cell clusters (termed microcolonies; see arrows Figure 1f-1) associated with a well-developed EPS matrix throughout the biofilm architecture. Along with the distinctive biofilm structural organization, the enamel hard surface also displayed different characteristics. Visually, the pattern of enamel demineralization in glucose+fructose appeared homogeneous, with opaque demineralized areas across the enamel surface (Figure 1a-2 and a-4).

Interestingly, the demineralization pattern in sucrose group was rather heterogeneous, showing localized areas of "white spot-like" demineralization on the enamel surface, which is similar to the early enamel carious lesions seen clinically (Figure 1a-1 and a-3). These visual differences were confirmed with surface roughness and microradiographic analyses of the enamel. The enamel from sucrose-grown biofilms developed rougher surface than that from glucose+fructose biofilms (Figure 1b). Importantly, the lesion depth as determined by microradiography demonstrated deeper demineralized lesions in the sucrose group (*vs* glucose+fructose; Figure 1c). Collectively, the data revealed that the formation microcolonies enmeshed in a well-developed EPS matrix in sucrose group resulted localized enamel demineralization with deeper lesion and rougher surface, showing a "white spots-like" pattern.

Spatial and structural organization of EPS and microcolony

Detailed *S. mutans* biofilm structure formed in 1% sucrose at 43 h was shown in Figure 1e, f-1, f-2 and f-3. Figure 1e displays the 3D rendering of the biofilm architecture, and cross sectional images illustrate bacterial cell clusters (Figure 1f-1) and EPS matrix (Figure 1f-2). Merged cross sectional images (Figure 1f-3) reveal that the microcolonies are surrounded by EPS forming compartmentalized yet interconnected microbial units of different sizes, which were found attached throughout the enamel surface. It is apparent that sucrose-mediated biofilm formation created spatial heterogeneities manifested by complex networks of EPS-surrounded microcolonies, forming an intricate structural framework providing support for localized bacterial accumulation and biofilm buildup. Excitingly, similar 3D architecture and presence of microcolonies (see arrows) were observed in sucrose-grown biofilms formed *in vivo* using the intra-oral human plaque model (Figure 2b). Close-up images show intricate and compartmentalized mixed-species bacterial cell clusters when plaque-biofilms were formed with sucrose (Figure 2c).

***In situ* pH distribution in biofilm structure**

The non-invasive 3D pH mapping allows spatio-temporal analysis of pH microenvironment within the biofilm and across the surface of attachment. The *in situ* pH distribution of *S. mutans* biofilms on the enamel surface is shown in Figure 3. Figure 3a displays the dynamic pH changes during neutralization by pH 7 buffer solution as well as the re-acidification of the biofilm environment following addition of glucose. The data indicated that EPS-enmeshed microcolonies were

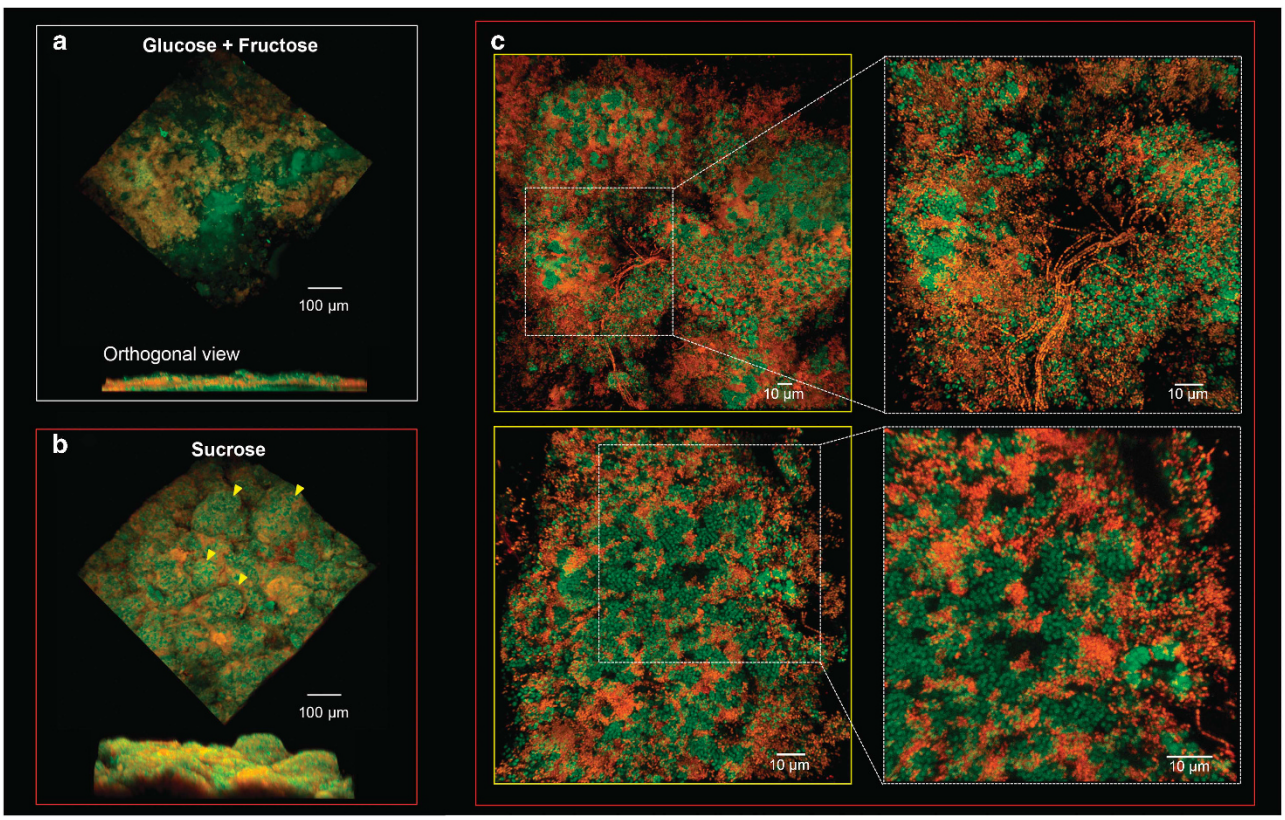

Figure 2 Intact mixed-species biofilms formed on teeth *in vivo* using the intra-oral (*in situ*) model. Representative 3D rendering images of plaque-biofilms formed in the presence of glucose+fructose (**a**) or sucrose (**b**). (**c**) Projection images of structured plaque-biofilms. All bacterial cells labeled with EUB338-Cy3 are depicted in green, while *Streptococcus* labeled with STR405-Cy5 is in red. Microcolonies (see yellow arrows) were observed in sucrose grown biofilms formed *in vivo* using the intra-oral human plaque model. (**c**) demonstrated the typical microlonies structure that were enlarged from (**b**).

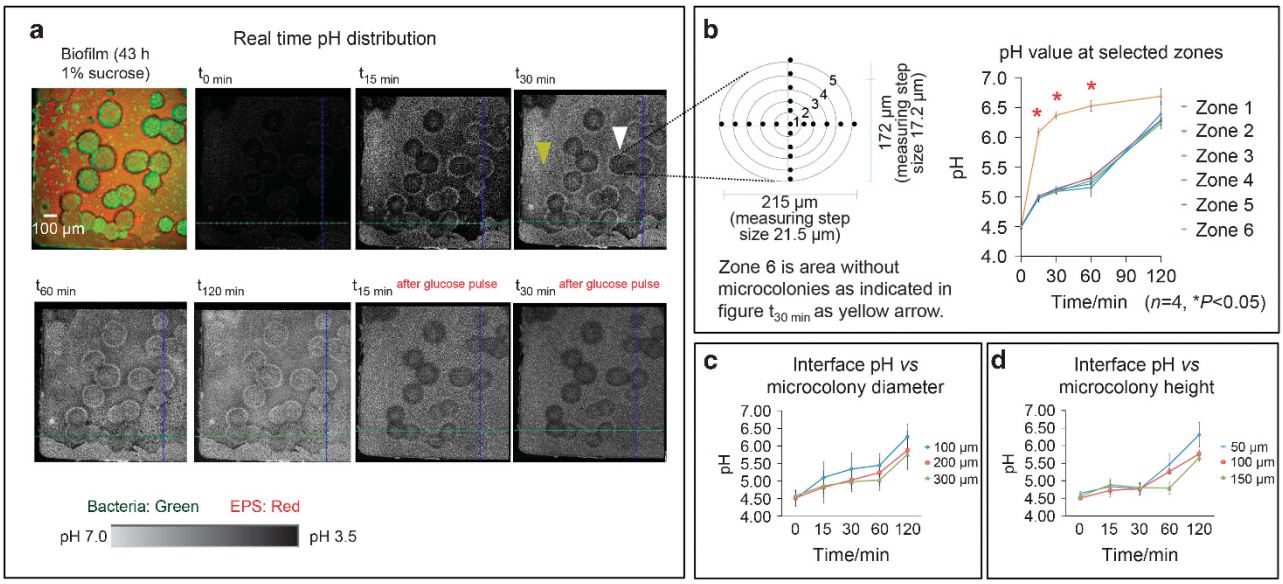

Figure 3 Biofilm structure and real-time pH profile. (**a**) Real-time pH distribution within biofilms; (**b**) pH value at selected zones within microcolony; (**c**) pH at the Interface between biofilm and enamel surface *vs* microcolony diameter; (**d**) pH at the Interface between biofilm and enamel surface *vs* height. EPS, exopolysaccharides.

resistant to neutralization by the buffering solution, particularly at biofilm/enamel interface. pH values at specific locations inside and outside of the microcolonies were determined over time as detailed in Figure 2b. Areas inside the microcolonies were divided into zone 1–5, while the area outside of microcolonies was named as zone 6. For regions located outside of microcolonies (zone 6), the pH rapidly increased to above 6 after 30 min incubation in neutral pH buffer. However, acidic regions (pH < 5.5) were detected in the interior of the microcolonies (zone 1–5), and persisted even after 60 min of buffer incubation; more than 120 min of neutral pH buffer exposure were required before neutralization ensues. This observation suggests that the presence of EPS-microcolony structure might be creating localized areas of resistance to neutralization and thereby delaying the buffering effect. Although we observed some variation of the pH values across the interior regions within the microcolonies, there were no significant differences between the various zones. Furthermore, glucose pulse after neutralization rapidly re-generated the acidic regions inside of microcolonies, indicating that glucose was utilized for acid production and the produced acids were accumulated within the microcolonies despite the presence of neutral pH buffer surrounding the biofilm.

EPS-enmeshed microcolonies size with the 3D dimensional pH distribution

The correlation between microcolonies diameter and the neutralization resistance at the interface between the biofilm and the enamel surface was examined and shown in Figure 2c. pH at the center of microcolonies with different diameters were selected for measurement. The results indicated that larger microcolonies were more resistant to neutralization, maintaining the biofilm pH under the critical demineralization point (pH 5.5) for prolonged period than those with smaller diameter.

DISCUSSION

In this study, we analyzed the influence of sucrose on the 3D architecture of intact biofilms formed on human tooth enamel, the spatial distribution of *in situ* pH and the dynamics of acidification within biofilm microenvironment. The data revealed that sucrose-grown biofilms were characterized by the presence of bacterial clusters (microcolonies) surrounded by an EPS-rich matrix. Furthermore, localized acidic pH values were confined in the interior of these microcolonies, which were highly resistant to neutralization. Interestingly, once neutralized, the acidic pH microenvironments were rapidly re-generated when glucose was provided to the biofilms. Importantly, the acidogenic biofilm structure was capable of causing substantial mineral loss and deep lesions on the enamel surface. This study provides a feasible explanation on how a complex 3D biofilm architecture help create localized acidic microenvironments in close proximity of the enamel surface, which promote the demineralization of tooth enamel.

Sucrose-mediated biofilm formation created spatial heterogeneities manifested by a complex network of microcolonies which modulate the development of compartmentalized acidic microenvironments across the 3D architecture. Furthermore, such structural organization was recapitulated *in vivo* when biofilms were formed intra-orally in the presence of sucrose. The maintenance of pH values below 5.5 in the interior of these EPS-embedded microcolonies is important because enamel starts to rapidly demineralize.[3] We found that acidic pH values at the tooth-biofilm interface were maintained under this critical point even after 60 min of incubation in neutral buffering solution, while the pH at the outside of microcolonies was readily neutralized (Figure 2b). As a result, regions of low pH value were confined at these specific locations, which could explain the appearance of white spot-like lesions pattern along the biofilm-enamel interface, leading to the elevated surface roughness as shown in Figure 1b. Notably, larger microcolonies maintained low pH values more effectively compared with smaller microcolonies, consistent with a recent report indicating an association between microcolony size and acidic pH values at the biofilm/apatite interface.[25] Thus, the prolonged period of enamel exposure to such acidic pH values within the enlarged microcolonies could more severely erode the apatitic surface. Indeed, white spot-like pattern was only visible on the enamel surface from sucrose-grown biofilms (Sm_{suc}-43 h and Sm_{suc}-67 h).

In contrast, biofilms formed with 0.5% glucose and 0.5% fructose (equivalent monosaccharide amounts of the disaccharide sucrose)

were incapable of forming organized bacterial clusters and were devoid of EPS-rich matrix. Consistent with previous observations,[26–27] the level of mineral loss and lesion depth was less pronounced than those formed in sucrose-biofilms despite the fact that these sugars can be metabolized by *S. mutans* into acids and cause demineralization. Furthermore, the pattern of demineralization was also different; a more homogeneous and opaque demineralized areas across the enamel surface were observed. Thus, it is conceivable that the presence of highly structured and enlarged EPS-enmeshed microcolonies created by sucrose utilization could retain produced acids at the enamel/biofilm interface more effectively than those from non-structured bacterial accumulation found in glucose+fructose-grown biofilms. A recent report also revealed that biofilms subjected to enzymatic degradation of the EPS matrix was readily neutralized by neutral pH buffer, and failed to maintain the acidic microenvironment in the interior of the microcolony.[25] The acids accumulated and confined in these specific areas of sucrose-grown biofilms could cause a more aggressive pattern of localized enamel demineralization and deeper lesions (*vs* glucose+fructose biofilms).

Clinical relevance

The development of highly structured bacterial microcolonies that are enmeshed in an EPS-rich matrix creates acidic regions at specific locations at the surface of biofilm attachment (despite exposure to buffered neutral pH). The presence of localized acidic pH regions at critical pH values on the enamel surface (associated with microcolonies) may serve as demineralizing sites for the onset of early carious lesions clinically known as "white spots". EPS-enmeshed microcolonies might be a potential "structural target" for anti-caries therapies aimed at controlling the assembly of virulent biofilms.

CONCLUSION

The simultaneous biofilm 3D architecture and pH distribution profiling revealed that the assembly of an EPS-rich matrix surrounding densely packed bacterial microcolonies may have an important role for the localized enamel demineralization, and thereby the initiation and severity of carious lesions. The formation of complex 3D architectures *via* sucrose utilization creates spatially heterogeneous yet localized acidic microenvironments that help maintain pH values under critical pH, particularly in close proximity of enamel surface. In turn, the maintenance of acidic pH values (<5.5) enhances the level of demineralization *in situ*, leading to the appearance of white spot- like lesions on the human tooth enamel surface.

ACKNOWLEDGEMENTS

This work was supported in part by the National Institute for Dental and Craniofacial Research (NIDCR) grants DE025728 (GH), DE18023 (HK) and DE25220 (HK).

1 Shah N. *Dental caries: the disease and its clinical management*, 2nd edn. Oxford: Blackwell Munksgaard, 2009: 498.
2 Ilie O, van Loosdrecht MC, Picioreanu C. Mathematical modelling of tooth demineralisation and pH profiles in dental plaque. *J Theor Biol* 2012; **309**: 159–175.
3 Bowen WH. The Stephan curve revisited. *Odontology* 2013; **101**(1): 2–8.
4 Igarashi K, Kamiyama K, Yamada T. Measurement of pH in human dental plaque *in vivo* with an ion-sensitive transistor electrode. *Arch Oral Biol* 1981; **26**(3): 203–207.
5 Newman P, MacFadyen EE, Gillespie FC *et al.* An in-dwelling electrode for *in-vivo* measurement of the pH of dental plaque in man. *Arch Oral Biol* 1979; **24**(7): 501–507.
6 Firestone AR, Imfeld T, Schiffer S *et al.* Measurement of interdental plaque pH in humans with an indwelling glass pH electrode following a sucrose rinse: a long-term retrospective study. *Caries Res* 1987; **21**(6): 555–558.
7 Belser U, Spörri S, Mühlemann HR. Uptake and retention of fluoride by intact and etched enamel. *Helv Odontol Acta* 1975; **19**(2): 69–71.
8 Imfeld T, Mühlemann HR. Cariogenicity and acidogenicity of food, confectionery and beverages. *Pharmacol Ther Dent* 1978; **3**(2/3/4): 53–68.
9 Vroom JM, De Grauw KJ, Gerritsen HC *et al.* Depth penetration and detection of pH gradients in biofilms by two-photon excitation microscopy. *Appl Environ Microbiol* 1999; **65**(8): 3502–3511.
10 Schlafer S, Raarup MK, Meyer RL *et al.* pH landscapes in a novel five-species model of early dental biofilm. *PLoS One* 2011; **6**(9): e25299.
11 Xiao J, Klein MI, Falsetta ML *et al.* The Exopolysaccharide matrix modulates the interaction between 3D architecture and virulence of a mixed-species oral biofilm. *PLoS Pathog* 2012; **8**(4): e1002623.
12 Guo L, Hu W, He X *et al.* investigating acid production by *Streptococcus mutans* with a surface-displayed pH-sensitive green fluorescent protein. *PLoS One* 2013; **8**(2): e57182.
13 Gashti MP, Asselin J, Barbeau J *et al.* A microfluidic platform with pH imaging for chemical and hydrodynamic stimulation of intact oral biofilms. *Lab Chip* 2016; **16**(8): 1412–1419.
14 Koo H, Xiao J, Klein MI *et al.* Exopolysaccharides produced by *Streptococcus mutans* glucosyltransferases modulate the establishment of microcolonies within multispecies biofilms. *J Bacteriol* 2010; **192**(12): 3024–3032.
15 Xiao J, Koo H. Structural organization and dynamics of exopolysaccharide matrix and microcolonies formation by *Streptococcus mutans* in biofilms. *J Appl Microbiol* 2010; **108**(6): 2103–2113.
16 Klein MI, Duarte S, Xiao J *et al.* Structural and molecular basis of the role of starch and sucrose in *Streptococcus mutans* biofilm development. *Appl Environ Microbiol* 2009; **75**(3): 837–841.
17 Klein MI, Xiao J, Heydorn A *et al.* An analytical tool-box for comprehensive biochemical, structural and transcriptome evaluation of oral biofilms mediated by *mutans Streptococci*. *J Vis Exp* 2011, (47): e2512.
18 DePedro HM, Urayama P. Using LysoSensor Yellow/Blue DND-160 to sense acidic pH under high hydrostatic pressures. *Anal Biochem* 2009; **384**(2): 359–361.
19 Hunter RC, Beveridge TJ. Application of a pH-sensitive fluoroprobe (C-SNARF-4) for pH microenvironment analysis in *Pseudomonas aeruginosa* biofilms. *Appl Environ Microbiol* 2005; **71**(5): 2501–2510.
20 Creeth JE, Kelly SA, González-Cabezas C *et al.* Effect of toothbrushing duration and dentifrice quantity on enamel remineralisation: an *in situ* randomized clinical trial. *J Dent* 2016; **55**: 61–67.
21 Paes Leme AF, Bellato CM, Bedi G *et al.* Effects of sucrose on the extracellular matrix of plaque-like biofilm formed *in vivo*, studied by proteomic analysis. *Caries Res* 2008; **42**(6): 435–443.
22 Zero DT. *In situ* caries models. *Adv Dent Res* 1995; **9**(3): 214–230.
23 Thurnheer T, Gmür R, Guggenheim B. Multiplex FISH analysis of a six-species bacterial biofilm. *J Microbiol Methods* 2004; **56**(1): 37–47.
24 Kim D, Sitepu IR, Hashidoko Y. Induction of biofilm formation in the betaproteobacterium *Burkholderia unamae* CK43B exposed to exogenous indole and gallic acid. *Appl Environ Microbiol* 2013; **79**(16): 4845–4852.
25 Hwang G, Liu Y, Kim D *et al.* Simultaneous spatiotemporal mapping of *in situ* pH and bacterial activity within an intact 3D microcolony structure. *Sci Rep* 2016; **6**: 32841.
26 Cury JA, Rebelo MA, Del Bel Cury AA *et al.* Biochemical composition and cariogenicity of dental plaque formed in the presence of sucrose or glucose and fructose. *Caries Res* 2000; **34**(6): 491–497.
27 Paes Leme AF, Koo H, Bellato CM *et al.* The role of sucrose in cariogenic dental biofilm formation—new insight. *J Dent Res* 2006; **85**(10): 878–887.

This work is licensed under a Creative Commons Attribution-NonCommercial-NoDerivs 4.0 International License. The images or other third party material in this article are included in the article's Creative Commons license, unless indicated otherwise in the credit line; if the material is not included under the Creative Commons license, users will need to obtain permission from the license holder to reproduce the material. To view a copy of this license, visit http://creativecommons.org/licenses/by-nc-nd/4.0/

© The Author(s) 2017